
Test beam Analysis of Silicon Strip Detector Prototypes for the ATLAS Inner Detector

DESY Summer Student Programme, 2021

Ankur Giri

Chandigarh University

Supervisor

Jan-Hendrik Arling



September 8, 2021

Abstract

The aim of the project is to study the performance of device and its efficiency, with the help of package called corrvreckan. The work implies offline analysis and reconstruction of team beam data that has been acquired using the help of EU-DET type telescopes at the DESY II test beam facility. The specific studied source is the non-radiated silicon strip detector termed as ITK timing plane and the study focusses on analyzing the hit detection efficiency of the device under test.

Contents

1 Introduction

- 1.1 DESY II
- 1.2 The Test Beam
- 1.3 EUDET-type telescope
- 1.4 EU-DAQ Framework

2 Software Packages

3 Methodology and Results

4. Conclusion

Acknowledgement

References

1 Introduction

Silicon solid state detectors are getting popular with every passing day. While these detectors come in different types of arrangement the most common reason for their popularity is the abundant availability of silicon and the efficiency of the electron to carry a signal. The following components listed below play a vital role in testing of these detectors:

- Test Beam
- EU-DET telescope
- EUDAQ Framework
- Corryvreckan

1.1 DESY II

DESY II offers test beam facility infrastructure in Hamburg Bahrenfeld and it has three independent beam lines with particles such as electrons and positrons. This facility is 292.8 m long and has an average radius of 46.6 m. The facility also provides users with the beam of energy 1-6 GeV/c.

The beam lines are linked to the DESY II synchrotron, which normally operates electron beams with oscillation energies ranging from 0.45 to 6.3 GeV. This Test Beam Facility is one of only a handful in the world that provides users with access to multi-GeV beams. It has the necessary infrastructure for the creation and testing of nuclear and particle physics detectors, as well as generic detector research and development.



Fig-1 DESY II Test Beam Facility

1.2 TEST BEAM GENERATION

Instead of employing a direct extraction of the primary beam in DESY II, the test beams are created through a twofold conversion in the DESY II Test Beam Facility. Bremsstrahlung photons are first produced by a fiber target in the DESY II beam orbit. These photons collide with the secondary target, producing electron/positron pairs. The test beam particles reaching the test beam regions are electrons or positrons with a particular momentum, depending on the polarity and strength of the magnetic field of the following dipole magnet. There are three separate beam lines known as TB21, TB22, and TB24, which are named by the locations of the principal targets situated behind the quadrupoles QF21, QF22, and QF24 accordingly. Our experiment utilizes the test bed 22.

As depicted in the figure 2. the electrons and positrons are then sent via a dipole magnet, which allows the particle energy and momentum to be selected based on the polarity and intensity of the field. The particles are subsequently collimated by the controlled primary collimator as they pass through an evacuated beam pipe. The test beam particles enter the Hall 2 test beam regions after going through the beam shutter. An exchangeable fixed size secondary collimator, as well as shielding devices functioning as beam dumps, are placed within the beam regions.

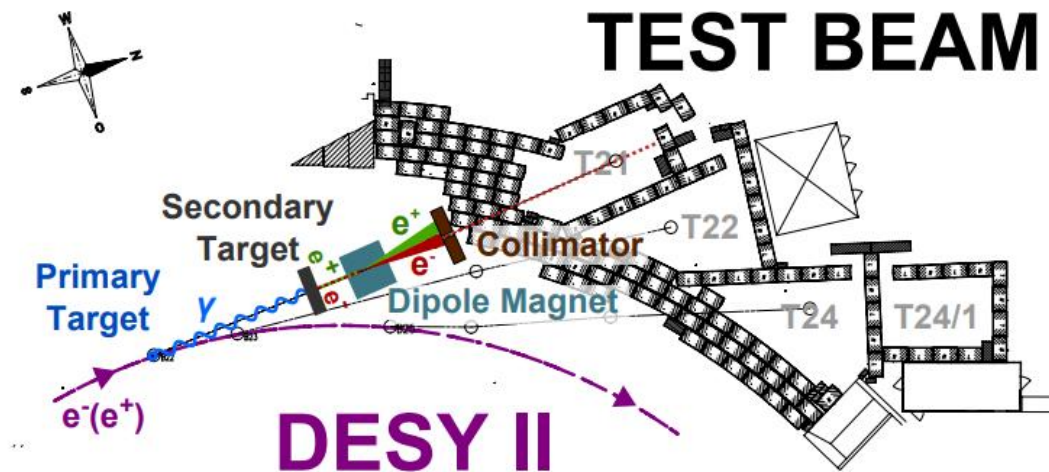


Figure 2: DESY II TEST BEAM GENERATION

1.3 EUDET- TYPE TELESCOPE

EUDET-Type telescopes are beam type telescope and plays a vital role in studying photo sensitive particle detectors. This telescope consists of six-pixel detector planes that are equipped with mimosa 26 monolithic sensors, mechanism for positioning of the telescopic planes, device. It also has a Trigger Logical Unit (TLU) that further helps in data acquisition system with trigger related tasks. The telescope planes are designed and manufactured with a modest material budget in mind in order to obtain high track resolution even at particle energies as low as 6 GeV at the DESY test beam facilities.

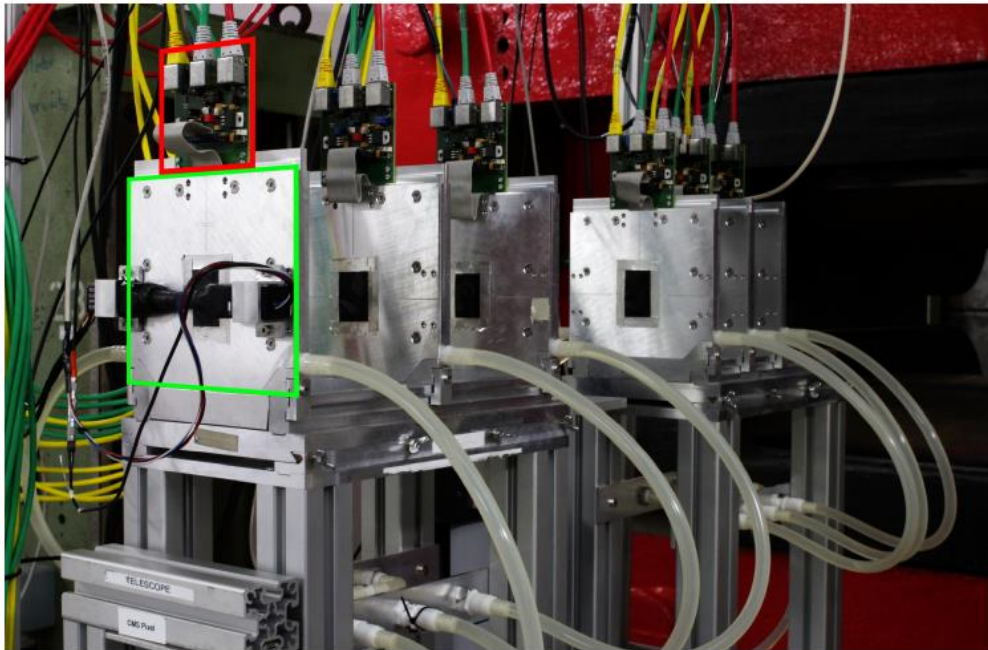


Figure 3: EUDET-TYPE TELESCOPE

The sensor planes of the DATURA beam telescope are mounted on aluminum rails as shown in the figure 3. The auxiliary boards containing clock, sensor settings, and data connections are placed on the aircraft' tops. Tubes deliver coolant to the planes. Each MIMOSA 26 sensor consists of pixels sized $18.4 \mu\text{m} \times 18.4 \mu\text{m}$, which are arranged in 1152 columns and 576 rows. The planes are divided into 2 telescopic arms, each with three sensors. The MIMOSA 26 sensors are read out with a rolling-shutter, taking 16 cycles of an 80 MHz clock per row, with all columns being read out in parallel. A DUT can be placed between the arms of the beam telescope or at either end. The telescope follows the right-hand side coordinate system where the y-direction points vertically down and the z-direction along the beam direction.

1.4 EUDAQ Framework

EUDAQ is a cross platform data acquisition framework which is designed to make data taking simple to use from the EU-DET type beam telescopes. The framework consists of three important systems: run control, producers and data collectors. Producers are responsible for delivering actual detector data to the framework. Producers are the interfaces between the EUDAQ architecture and subdetector systems such as beam telescopes, TLUs, and user DAQ devices. They communicate with the EUDAQ library and offer a set of commands that the Run Control can use. This straightforward interface design makes it easier to integrate user DAQ equipment into the software framework. The data collected from the detectors by the separate Producers is transmitted to the Data Collector. This Data Collector is in charge of event construction, which is the correlation of events from all subdetector systems to single global events that include all data relating to a single trigger.

The Online Monitor tool is provided to guarantee data quality during data gathering. It connects to the Data Collector and requests a specified proportion of the recorded events (for example, one out of a hundred) to fully decode all subdetector data and produce simple graphs such as hit maps or correlation plots. As a result, data quality monitoring is available during data collection to ensure that the various instruments are synced in time and all fall within the geometrical trigger acceptability.

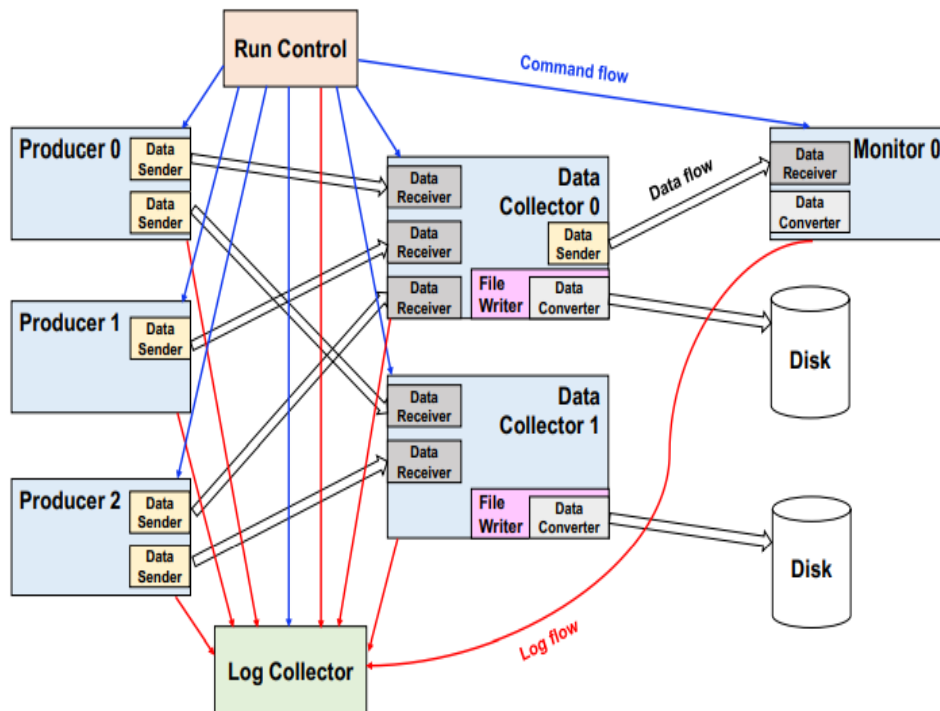


Figure 4: EUDAQ FRAMEWORK

2 Software Packages

There are mainly two important packages that have been used throughout this project mainly `corrvreckan` which is used to reconstruct the analysis from the offline data files and `root` which is used to analyze the plots saved by `corrvreckan` in the form of root files.

2.1 CORRVRECKAN

`Corrvreckan` is a test beam data reconstruction framework that is versatile, quick, and lightweight, based on a modular reconstruction chain idea. It is developed in contemporary C++, has few other dependencies, and is intended to be freely customizable by the user without requiring code changes.

The reconstruction chain's modularity allows users to add their own functionality (such as event loaders to support different data formats or analysis modules to investigate specific detector features) without having to deal with centrally provided functionality such as coordinate transformations, input and output, parsing of user input, and analysis configuration.

It is also possible to combine the usage of both software frameworks: data produced by EUDAQ framework can be read in and analyzed with `Corrvreckan`. This allows, for instance, to perform data comparisons when simulating a beam telescope configuration and analyzing it with the same parameters as the read test-beam data.

```
Corrvreckan v2.0+303^g7746ea7
The Maelstrom for Your Test Beam Data

Usage: corry -c <config> [OPTIONS]

Options:
  -c <file>      configuration file to be used
  -l <file>      file to log to besides standard output
  -o <option>    extra configuration option(s) to pass
  -g <option>    extra detector configuration options(s) to pass
  -v <level>    verbosity level, overwriting the global level
  --version     print version information and quit
[agiri@lxplus748 agiri]$ |
```

Figure 5: Corrvreckan Interface

`Corrvreckan` works in terms of modules read from a configuration file and an event loop that processes data from all detectors allocated to one event sequentially. All modules are performed in the order they appear in the configuration file during each loop iteration and have access to all data produced by preceding modules. The data cache is emptied at the conclusion of the loop iteration, and the framework moves on to the next iteration.

It works on two configuration files as shown in figure 6 and figure 7 one is used to declare all the modules that are needed for the reconstruction chain and the other provides the information about the geometry of the detectors and their specification.


```

<1> agiri@lxplus743...

[Corrvvreckan]
log_level = "INFO"
log_format = "DEFAULT"
log_file = 'logs/log_corrv'

detectors_file = "geometries/01_mask_geo.conf"
#detectors_file = "02_prealign.conf"
detectors_file_updated = "02_prealignmimosa.conf"
#Following histogram_file is the filename where root histograms get saved, usually defined in scripts
histogram_file = "beforeprealignmimosa.root"

output_directory = "output"
# Number of events to be processed
number_of_events = 10000

[EventLoaderEUDAQ2]
name = "TLU_0"
get_time_residuals = true
file_name = "/eos/atlas/atlascerngroupdisk/det-itk/general/strips/Testbeam/June2021/synced_data/sync003284.raw"
adjust_event_times = [{"TLURawDataEvent", -1us, +1us}]

[EventLoaderEUDAQ2]
file_name = "/eos/atlas/atlascerngroupdisk/det-itk/general/strips/Testbeam/June2021/synced_data/sync003284.raw"

[ClusteringSpatial]
charge_weighting = false
use_trigger_timestamp = true
#type = "MIMOSA26"

"02_initial.conf" 79L, 4415C

```

Figure 6: Config file

```

<1> agiri@lxplus743...

[TLU_0]
orientation = 0,0,0
orientation_mode = "xyz"
position = 0,0,0
role = "auxiliary"
time_resolution = 1s
type = "tlu"

[MIMOSA26_0]
material_budget = 0.00075
number_of_pixels = 1152, 576
orientation = 0,0,0
orientation_mode = "xyz"
pixel_pitch = 18.4um,18.4um
position = 0,0,0
spatial_resolution = 4um,4um
time_resolution = 230us
type = "mimosa26"
role = "reference"

[MIMOSA26_1]
material_budget = 0.00075
number_of_pixels = 1152, 576
orientation = 0,0,0
orientation_mode = "xyz"
pixel_pitch = 18.4um,18.4um
position = 0,0,105.5mm
spatial_resolution = 4um,4um
time_resolution = 230us
type = "mimosa26"

[MIMOSA26_2]
material_budget = 0.00075
number_of_pixels = 1152, 576
orientation = 0,0,0
orientation_mode = "xyz"
"01_initial_geo.conf" 104L, 2920C
ssh.exe*[64]:25900

```

Figure 7: Geometry file

2.2 ROOT

ROOT is a high-energy particle physics data processing software program created at CERN. It includes all of the features required for 'big data' and statistical analysis, as well as visualization ('plotting') and data storage. As a result, it is utilized not just in particle physics but also in other disciplines of research and even industry, and many plots you may have seen in lectures or publications, such as the famous Higgs discovery plots, have been created using ROOT. As high-performance software, ROOT is written mainly in C++.

```
> <1> agiri@lxplus782...
[agiri@lxplus782 agiri]$ root
-----
| Welcome to ROOT 6.24/04                                     https://root.cern |
| (c) 1995-2021, The ROOT Team; conception: R. Brun, F. Rademakers |
| Built for linuxx86_64gcc on Aug 25 2021, 12:59:28           |
| From tags/v6-24-04@v6-24-04                               |
| With c++ (GCC) 4.8.5 20150623 (Red Hat 4.8.5-44)           |
| Try '.help', '.demo', '.license', '.credits', '.quit'/'.'q' |
|-----|
root [0] |
```

Figure 8: Root Interface

Apart from this there is also a sub component/ class of root known as TBrowser which has been used in this project for analyzing the results graphically.

All ROOT objects can be browsed using a TBrowser. It displays all browsable ROOT classes in a list on the left side of the window. When you choose one of the classes, all of the items in that class are displayed in the icon box on the right side. Selecting one of the items in the icon box will create a new list of all browsable objects and render the contents of the selected class in the icon box.

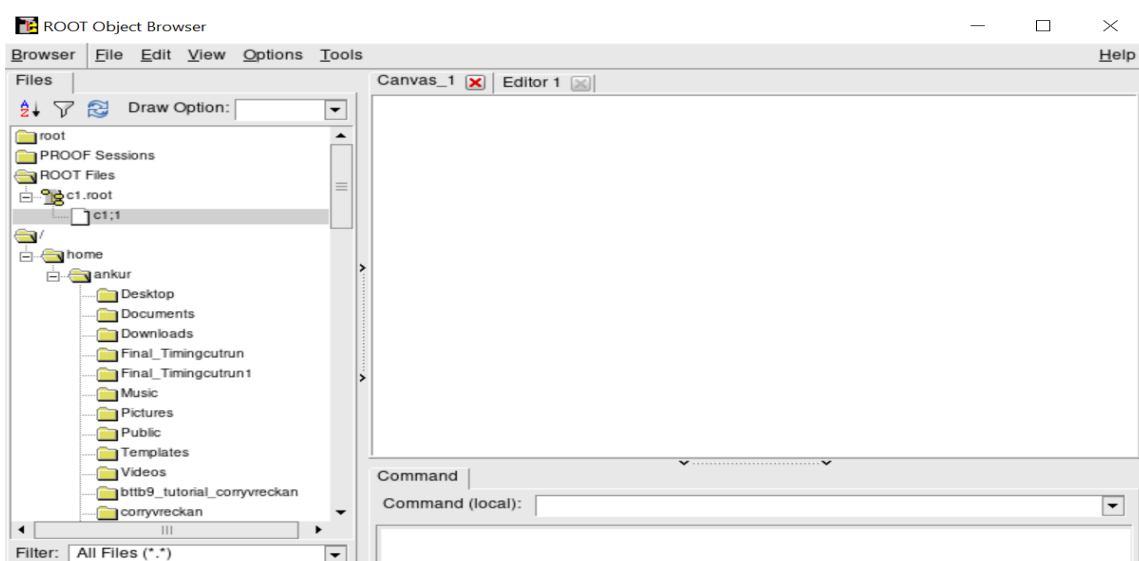


Figure 9: TBrowser

3 Methodology and Results

The reconstruction of test beam data in Corryvreckan consists of many steps as shown in the figure 10. below from loading the collected data using event loader to dut analysis in the end the section below will go through all the steps one by one.



Figure 10: Reconstruction chain for test beam

3.1. Reading in of Raw Data

Data collected during a test-beam campaign is often kept in binary files rather than tables, i.e., in a non-human-readable manner. As a result, the initial stage in the reconstruction process is to extract the raw data from the file and interpret portions of the data stream as pixel hit information. This is done in Corryvreckan modules named **EventLoaderDetector Name**. In our case we use the detector name **EUDAQ2**.

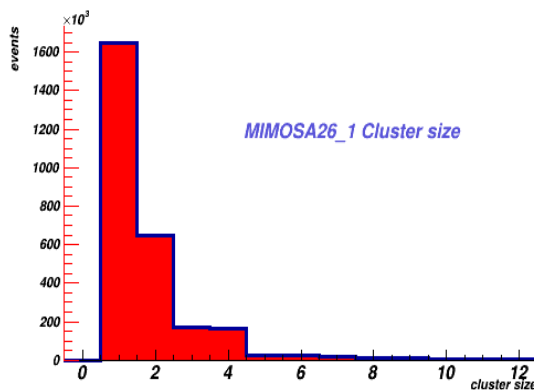
3.2. Spatial Clustering

A travelling particle may produce electron-hole pairs in two or more neighboring pixels depending on the incident location and angle. Furthermore, through lateral diffusion, charge can "leak" from one pixel into neighboring cells. This is referred to as charge sharing.

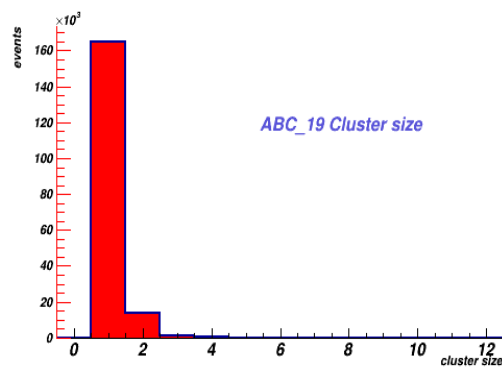
Clustering Spatial clusters, a detector's incoming data in the absence of distinct hit timestamps the clustering technique solely employs positional information: either charge-weighted center-of-gravity or arithmetic mean computation using the touching neighbor's method, and no time information is included.

For every detector this module produces two types of plots:

- A two-dimensional map of the cluster locations in global and local coordinates.
- Cluster size, charge, seed charge, width in X and Y, timestamps, and multiplicity histograms



Cluster Size Plot for Mimosa_1



Cluster Size Plot for DUT

3.3. Correlations

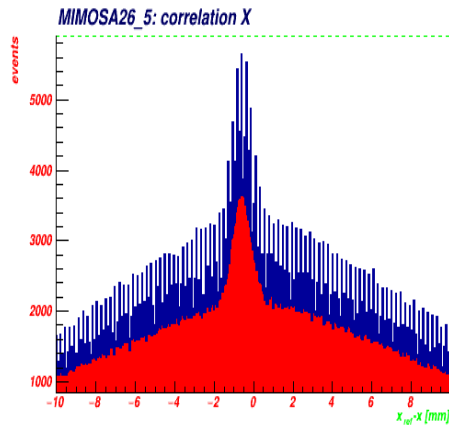
In the context of test-beam reconstruction, spatial correlations can be specified at the pixel or cluster level. In this scenario, the spatial correlations and histograms are calculated as follows:

X correlation = x cluster on **reference** detector – x cluster on **this** detector

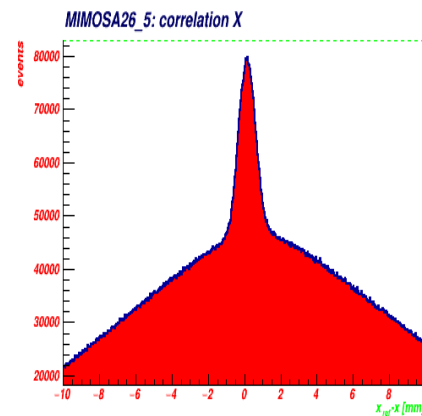
Y correlation = y cluster on **reference** detector – y cluster on **this** detector

For all sensors, the raw data only contains basic pixel hit information. As a result, the reconstruction software is unaware of the precise location of the sensor planes. As a result, to define the location and rotation of all detectors, a detector geometry file is required. While the location we provide in the geometry file are only measured by hand to a precision of 1mm only and hence they can be different from the ideal position of all the planes. Hence, we use alignment procedures by software to find the ideal position of the individual plane and this helps in reducing the offsets of multiple pixel hits further while reconstruction of tracks.

Calculating correlations is easy as it can be calculated from raw data and doesn't need any tracking. Furthermore it also gives us an initial estimation of the alignment of the sensor planes and the device. The peaks are clearly visible in the spatial plot of all sensor planes for X and Y axis for a perfect pre alignment they should peak around zero.



Plot-Before Pre-alignment



Plot-After Pre-Alignment

In the plots above we can see that before using the pre-alignment module our correlation peaks for one of the sensor planes were not properly aligned to zero but after running the software-based alignment the peaks are nicely aligned to zero.

3.4. Tracking

The next step after doing the realignment is to make tracks. Clusters on the planes of the reference telescope that are within a particular spatial and time interval are merged into a straight-line track for tracking. To eliminate bias in the analysis, the DUT plane should be removed from tracking. For this more detailed tracking we use the residual's plots. A spatial residual plot depicts the difference between the interpolated track intercept onto a certain plane and the position of the cluster on that plane. There are two types of residuals unbiased residuals and the other is biased residuals.

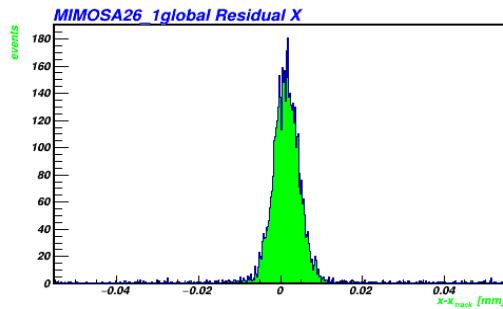
For biased residual, the cluster on the plane is part of the track and unbiased residuals, are those in which the cluster has been associated to the track after the track fitting and is not part of the track itself.

The residuals for X plane are calculated from the formula below:

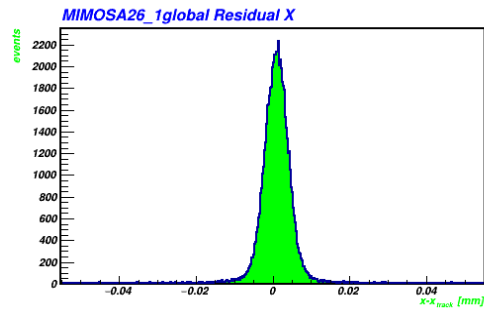
Biased: X residual = x track intercept on this plane - x track cluster on this plane

Unbiased: X residual = x track intercept on this plane - x associated cluster on this plane

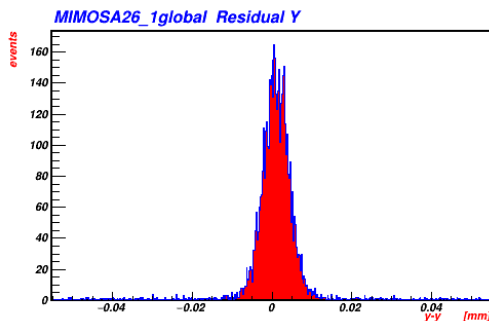
With this same formula the residuals in Y directions are also calculated. Just like pre-alignment from correlations the the goal of the alignment is to force the residuals to be centered around zero.



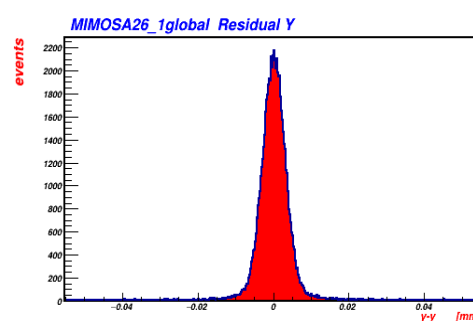
Plot: X Residuals before alignment



Plot: X Residuals after alignment



Plot: Y Residuals before alignment



Plot: Y Residuals after alignment

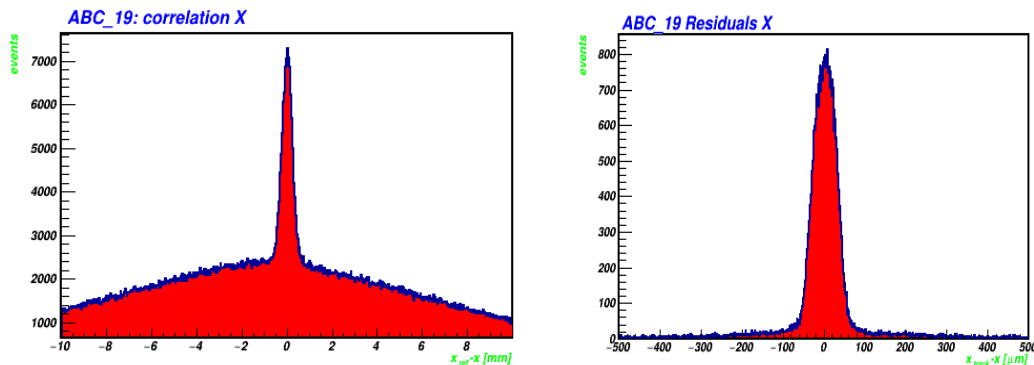
As one can notice that above plots x residuals peak was slightly off in the right-hand side zero of x axis which then got corrected by the **[AlignmentTrackChi2]** module which does the alignment iteratively. The same symmetry is also shown below for the y plane of the mimosa sensor.

3.5. DUT Association

After completing the telescopic alignment for the all the mimosa planes its now time to align the DUT before it gets associated with the tracks. Since the DUT is excluded from the tracking, the clusters on the DUT are not part of a track. We must associate the DUT's clusters with tracks in a different method. To accomplish so, we employ the **DUTAssociation** module. It computes the track intercept with the DUT for each track and looks for clusters within a given spatial and time range that might be connected with this track. In addition, the module **AnalysisDUT** can be used to calculate the DUT residuals. But before doing all these we need to do the pre-alignment of the DUT as well just like the telescopic planes with the help of correlation plots.

After completing the pre-alignment, the module **AlignmentDUTResidual** is utilised, which repeatedly changes the DUT's location and rotation to centre the unbiased residuals in x and y around zero and reduce their widths.

Below are some corrected correlation plots and residuals plots after aligning the DUT

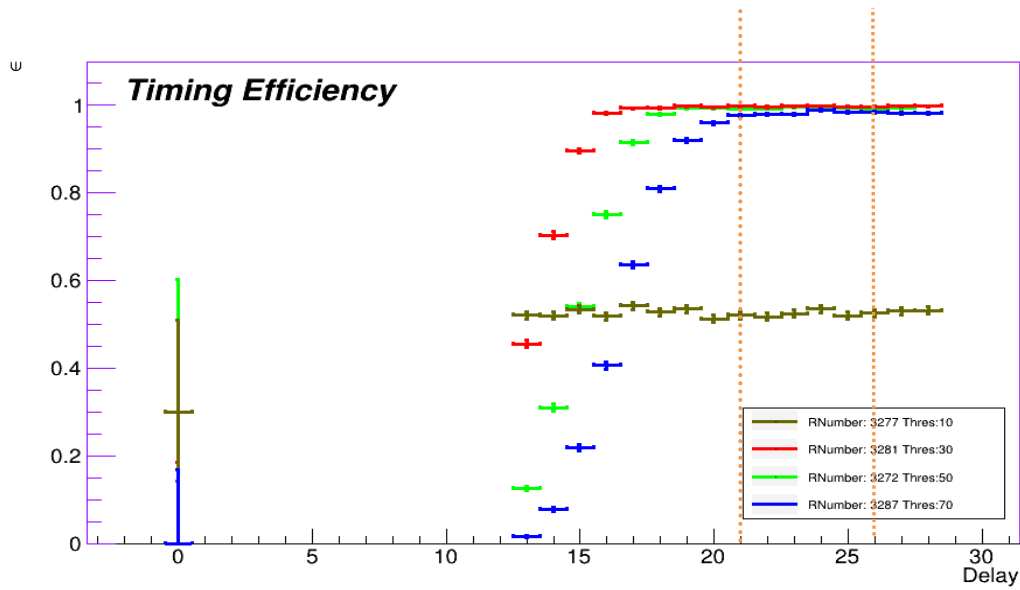


Plot showing corrected correlation peak for DUT ABC 19 Plot showing corrected residual peak for DUT ABC 19

3.6. DUT Analysis

After fully aligning the telescope and associating the DUT properly it's time to do the analysis of the device in which we can investigate the performance of the device. For reliable analysis results, it is important to have a high number of tracks for good statistics.

For this we utilized the entire data set using the custom module named as **AnalysisItkStripEfficiency** with a delay cut window 24, 12 on four different threshold such as 10,30,50 and 70. Running this analysis for different threshold gave us the following timing efficiency plot as shown below.



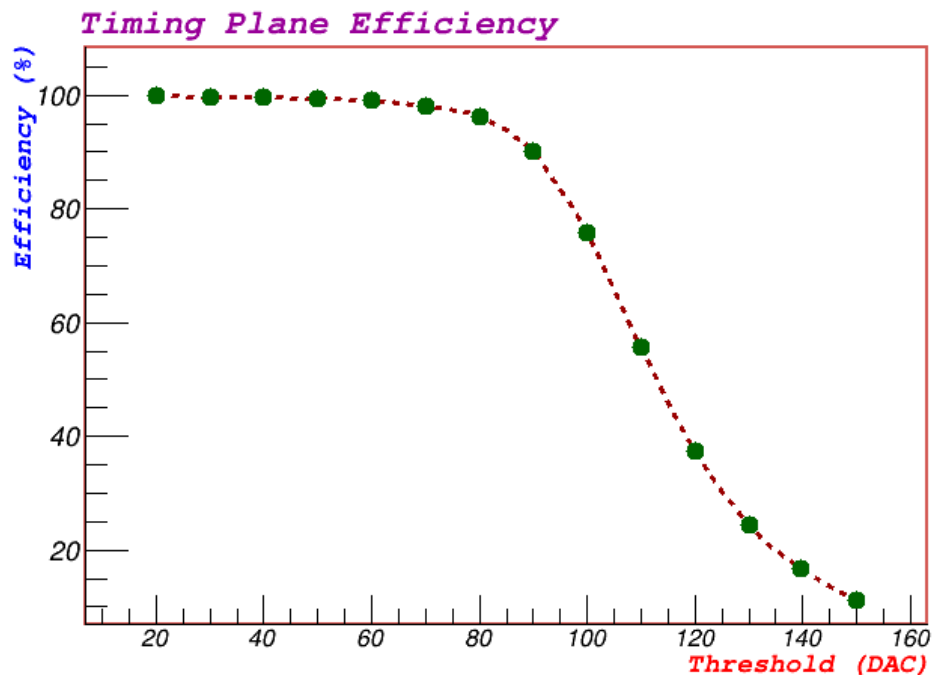
Plot : Timing efficiency plot for different threshold run

As depicted in the plot above we can notice that we reach highest efficiency for delay cuts 21 to 26. The delay might be there for the fact that the beam takes some time to travel from the first plane to the dut. Further other reason could be because of the delay that is there in the electronics such as triggering, control lines etc.

It is important to note that here for threshold less than 20 the efficiency of this particular batch of devices are really low and it reaches efficiency higher than 90 only for threshold more than 20. The main reason could be because of the noises that are there in the low threshold runs.

4 Conclusions

After deciding on the delay cuts , re-running the analysis for every threshold in steps of ten and plotting the efficiency vs threshold gives us an expected S-curve as depicted in the plot below.



Plot: Device Efficiency Plot

We managed to get smooth and homogeneous S-curve combining all the threshold. Despite all the noises present at this point of the investigation we managed anyway to see what we expected after aligning the telescope and DUT. In the future analysis the aligned geometric files can be used to run over the other threshold as well.

Acknowledgements

I want to first thank DESY that have given me the opportunity to work for two months with the ATLAS group and also for the online lecture's experiences. I also want to thank my supervisor **Jan-Hendrik Arling** that gave me this interesting project and helped me with all the concept building and clearing my doubts whenever I was stuck at some part of the project. I could have not achieved the results without his supervision.

References

- [1] R. Diener et al., "The DESY II test beam facility", *Nuclear Instruments and Methods in Physics Research Section A: Accelerators, Spectrometers, Detectors and Associated Equipment*, vol. 922, pp. 265-286, 2019. Available: [10.1016/j.nima.2018.11.133](https://doi.org/10.1016/j.nima.2018.11.133).
- [2] D. Dannheim et al., "Corryvreckan: a modular 4D track reconstruction and analysis software for test beam data", *Journal of Instrumentation*, vol. 16, no. 03, p. P03008, 2021. Available: [10.1088/1748-0221/16/03/p03008](https://doi.org/10.1088/1748-0221/16/03/p03008).
- [3] J. Arling, "The ATLAS Strip Detector System for the High-Luminosity LHC", 2019.
- [4] CERN. Geneva. The LHC experiments Committee, "Technical Design Report for the ATLAS Inner Tracker Strip Detector", 2017.
- [5] H. Jansen et al., "Performance of the EUDET-type beam telescopes", *EPJ Techniques and Instrumentation*, vol. 3, no. 1, 2016. Available: [10.1140/epjti/s40485-016-0033-2](https://doi.org/10.1140/epjti/s40485-016-0033-2).